STATE RESEARCH CENTER OF RUSSIA

INSTITUTE FOR HIGH ENERGY PHYSICS

IHEP 2000-42

A.A. Bogdanov[1], S.B. Nurushev[2], M.F. Runtzo[1],
M.N. Strikhanov[1], A.N. Vasiliev[2]

THE LOCAL INCLUSIVE PHOTON POLARIMETER FOR RHIC

[1] Moscow Engineering Physics Institute (Technical University), Kashirskoe Av. 31, 115409, Moscow, Russia
[2] Institute for High Energy Physics, 142284 Protvino, Russia

Protvino 2000

UDK 539.1.07 M–24

Abstract

Bogdanov A.A., Nurushev S.B., Runtzo M.F., et al. The Local Inclusive Photon Polarimeter for RHIC: IHEP Preprint 2000-42. – Protvino, 2000. – p. 17, figs. 9, tables 6, refs.: 13.

The local inclusive photon polarimeter with full azimuthal coverage is proposed for continuous monitoring of the beam transverse polarizations at RHIC top energy. Since the used beams are mostly longitudinally polarized, the photon detector by measuring the transverse components of the polarization vector is able to determine a stable polarization direction in space. The tracking detector may be used for the vertex reconstruction of photons. For calibration of this polarimeter it is foreseen to install a jet or foil target in the rear part of the main detector, for example, PHENIX. Several sources of backgrounds are revealed and possible ways of their suppressions are discussed. Space limitations and magnetic field of the main experimental setup impose severe restrictions up on the position and shape of the local inclusive photon polarimeter, which were taken into account.

Аннотация

Богданов А.А., Нурушев С.Б., Рунцо М.Ф. и др. Локальный инклюзивный фотонный поляриметр для RHIC: Препринт ИФВЭ 2000-42. – Протвино, 2000. – 17 с., 9 рис., 6 табл., библиогр.: 13.

Для непрерывного мониторирования поперечных поляризаций пучков при верхней энергии RHIC предлагается использовать локальный инклюзивный фотонный поляриметр с полным азимутальным перекрытием. Так как используемые пучки большей частью являются продольно-поляризованными, то фотонный детектор путем измерения поперечных компонент вектора поляризации может определить стабильное направление вектора поляризации в пространстве. Трековый детектор может применяться для восстановления фотонной вершины. Для калибровки такого поляриметра предусматривается установка струйной мишени или фольги на выходе пучка из детектора, например, PHENIX. Определены несколько источников фонов и обсуждаются возможные способы их подавления. Пространственные ограничения и магнитное поле установки предъявляют серьезные требования к детектору и они учитываются при создании инклюзивного фотонного поляриметра.

Introduction

The comprehensive Spin Physics Program was approved at RHIC [1] and the corresponding technical developments for creating the polarized proton beams up to the RHIC top energy are underway [2]. As regards the polarimetry, the most effort is directed toward the construction of the polarimeter of general use, that is, for measuring the beam polarizations in some fixed and convenient places in the rings [2]. But the detectors like PHENIX and STAR need to have the local polarimeter monitoring of the beam polarization at the interaction point (IP). Moreover, since the useful beam is longitudinally polarized, the local polarimeter should be able to show that at IP the beam has not any transverse component of the polarization vector. Up to now we did not know any attempt of building such a local polarimeter, an exclusion is K.Imai's suggestion to insert the photon polarimeter for PHENIX inside the muon piston [3]. We pursued such suggestion, but encountered several problems. Firstly, a huge background is expected from softer π^0 decays, not carrying any analyzing power. Secondly, the polarimeter run will be destructive in the sense, that the main physics run should be interrupted in the case of the polarimeter running. Thirdly, no possibility is foreseen to calibrate such a polarimeter. Taking into account these motivations, we propose for top RHIC energy the Local Inclusive Photon Polarimeter (LIPP) installed behind the DX magnet, at a distance $l_0 \simeq 18$ m from IP. Assuming that the analyzing power of the inclusive photon production does not depend on the initial energy, we show that LIPP is able to monitor the beam polarization simultaneously with the main run. A particular scheme is proposed to calibrate the LIPP. The background estimates are presented too.

This paper is compiled in the following way. Section 1 justifies the Local Inclusive Photon Polarimeter for main RHIC detectors like PHENIX. STAR, etc. Section 2 presents a scheme of polarimeter, its dimensions, position and interaction with the accelerator environment. Section 3 describes the concept of polarimeter and outlines some assumptions made in the following calculations. Section 4 is devoted to the Monte Carlo simulation of the polarimeter parameters at the Beam Colliding Mode (BCM) at $\sqrt{s} = 500$ GeV. Section 5 discusses the backgrounds coming from the neutral hadron productions, while Section 6 is devoted to another source of background caused by the beam-gas interaction. A possible way of the LIPP calibration by referring to the E704 data at 200 GeV/c in a fixed target mode is discussed in Section 7. The concluding section outlines the results of this study of the Inclusive Photon Polarimeter for PHENIX.

1. Why do we propose the inclusive photon polarimeter for PHENIX?

We assume that PHENIX will operate for Spin Physics in the following three distinct beam conditions:

- longitudinally polarized proton beams,
- transversally polarized proton beams, and
- unpolarized proton beams.

There are several reasons why only the inclusive photon reaction

$$p\uparrow + p \to \gamma + X, \tag{1}$$

may be used as a local polarimeter at PHENIX. Firstly, the photon is not influenced by the magnetic field of detector. Secondly, the photon can be easily identified by the electromagnetic calorimeter itself. Thirdly, and what is very important, the photon detector can have a full azimuthal coverage and such a property is crucial in defining the transverse components of the beam polarization. Fourthly, as is well known from the E704 results, for the reaction with inclusive π^0 and η productions (which are the main sources of photons)

$$p\uparrow + p \to \pi^0,\ \eta + X, \tag{2}$$

the analyzing power A_N is significant in the domain

$$0.4 < x_F < 0.8 \text{ and } 0.6 < p_T < 1.2 \text{ GeV/c}. \tag{3}$$

Let us denote those photons which originate from π^0 and η belonging to domain (3) as "useful" photons (they have the same analyzing power as their parents), while photons originating from the mesons not belonging to domain (3) as "harmful" photons (they have a zero analyzing power). Since π^0 and η-mesons have practically the same analyzing power, we may treat both of them as pions if otherwise is not stated clearly. Due to the restrictions (3) the "useful" photons should be also more energetic than the "harmful" photons. The principal way to suppress the background photons (including the "harmful" photons and photons from other sources) is to put a high threshold when detecting photons. That can easily be done in the electromagnetic calorimeter. An additional way to suppress the backgrounds is to detect the charged particles accompanying π^0 and $\eta-$ mesons and to reconstruct the event vertex with the precision of order of "diamond" region of the colliding beams. So, we argue that photon detection and identification offer some advantages over the charged particle detection and identification in this particular case of the local polarimetry.

Since we detect the inclusively produced photons originating from different sources, the measured analyzing power presents the weighted sum over all photons

$$A_N(\gamma) = \sum_{i=1}^{i=n} w(\gamma_i) \cdot A_N(\gamma_i), \tag{4}$$

where $w(\gamma_i)$ is a weight of source i, while $A_N(\gamma_i)$ is an analyzing power of that source. Examples, i=π^0, η , K^0, Λ, etc. $A_N(\gamma_i)$ are known from the experiment, like E704 at FNAL, while $w(\gamma_i)$ comes either from differential cross sections$\times$acceptance or from simulation as we shall do later.

2. Scheme of the Inclusive Photon Polarimeter

According to the PHENIX documentation [4] there is no space for installation of the photon polarimeter very close to the interaction point. In this situation we propose to install LIPP at a distance of $l_0 \simeq 18$ m from IP, just behind the beam deflection magnet DX (see Fig.1).

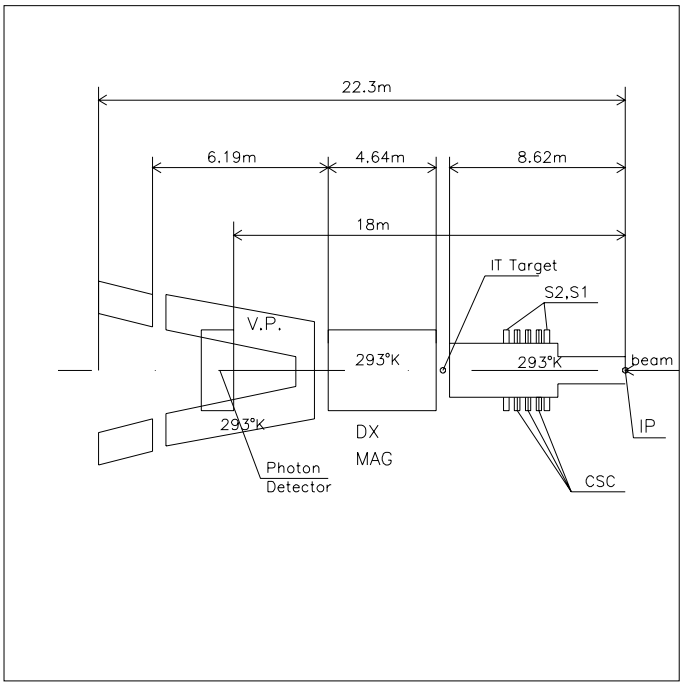

Fig. 1. The top view of the warm intersection region of RHIC. Photon Detector (PD) is installed at the distance of 18 m from the Interaction Point (IP). A space for PD is limited by the two beam pipes. The tracking detector, Cathode Strip Chambers (CSC), flanked by two scintillation counters for triggering, is shown too. The Internal Target (IT) for the PD calibration is positioned at l_{IT}=8.63 m from IP.

We know that in this place the Zero Degree Calorimeter (ZDC) is installed [5]. Therefore, our photon polarimeter should be installed just in front of the ZDC. The combination of PD and ZDC may be attractive for the suppression of the backgrounds from the neutral hadrons (see discussions below). The dimension and shape of the photon detector (PD) in a selected position is defined by the two beam pipes for the opposite moving protons. This can be seen in Fig.2. We selected an outer diameter of the PD as equal to $D_{out} = 220$ mm at the azimuthal angular region $\phi = 30^0 - 150^0$ and $\phi = 210^0 - 330^0$. At the angular interval $\phi = 330^0 - 30^0$ and $150^0 - 210^0$ the PD is cut in order to avoid any attachment to the beam pipes. Since the PD has a 90^0 symmetry, we made all calculations for the one sector from 30^0 to 90^0. The photon conversion on the walls of the pant like the vacuum pipe may arise another problem. It is preferable to transform this pipe to the skirt like a vacuum vessel in order to decrease the materials along the photon path. The aperture of the PD and its position define the maximum polar angle θ_{max}=110 mm/18 m=6.11 mrad accepted by the detector. In order to get the useful pions (3), we should keep the relation $E(\pi^0) \geq$(0.6 GeV/c)/6.11 mrad$\approx$100 GeV. Or $x_F \geq 100/250 = 0.4$. Two symmetrical photons emitted by π^0 with energy of 100 GeV will have half of π^0 energy,

that is, 50 GeV and their opening angle is equal to $\psi = 2 \cdot m_{\pi^0}/100$=2.7 mrad. At the PD this corresponds to their separation by a distance of 48.6 mm (at 18 m from IP). It means we have some chance to fit to domain (3) and at the same time to detect both decay photons separately. Therefore, we plan to detect single photons from any decay or both photons simultaneously in order to have a good apparatus efficiency. Also π^0 detection allows one to calibrate the energy resolution of PD.

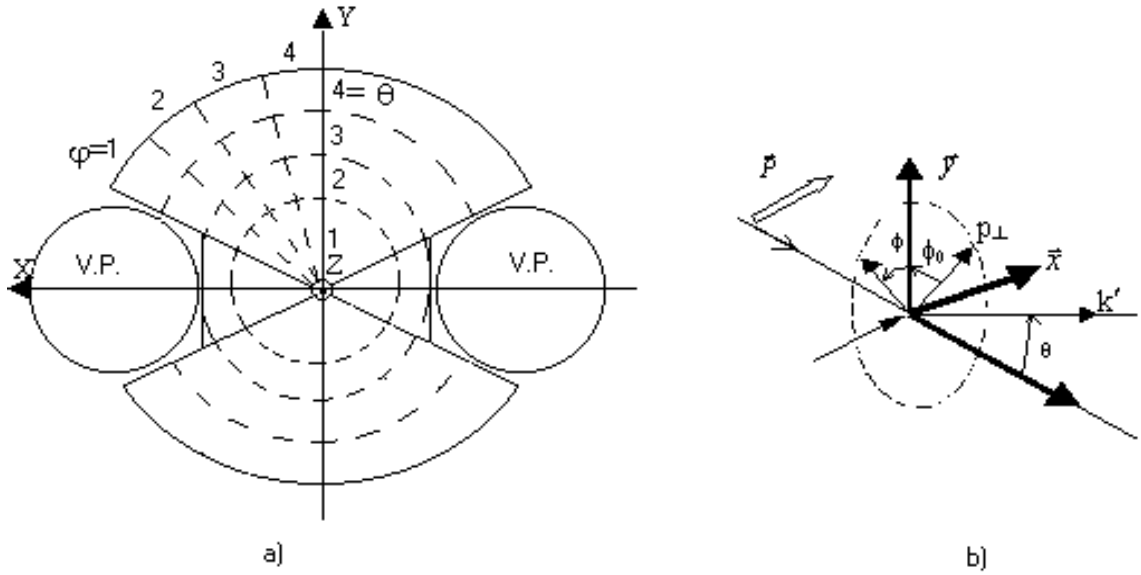

Fig. 2. The cross section of the photon detector showing its shape and the number of cells in (θ, ϕ) coordinates (left picture). One can also see the limitations due to the closeness of the two beam pipes. The coordinate system for inclusive photon production (right picture). $\vec{n}$ — the unit vector normal to the photon production plane, $\vec{P}_B$ — polarization vector, $P_\perp$ — its projection on to the (x,y) plane, inclined under angle ϕ_0 to the y-axis; k' — photon momentum defined by angles θ and ϕ.

Detection of both photons with a limited statistics may be useful for defining the analyzing power of inclusively produced π^0-mesons and comparison with E704 data. Additionally, having the selected π^0, one can check our assumption experimentally, that the photons have the same analyzing power as their parent particles.

Our scheme is correct for the RHIC top energy. For the lower energy, it is necessary to apply the technique proposed earlier in [6].

Above we have omitted the discussion of the scintillating counters surrounding the PD which might be used for triggering the PD.

3. Concept of the inclusive photon polarimeter

The possibility of applying the inclusive neutral pion polarimeter to the high energy accelerators/colliders was discussed in the previous papers [6], [7]. In the particular case of the PHENIX detector we are going to propose the local inclusive photon polarimeter as it was explained earlier. In the following we apply the technique proposed in [8] to the analysis of the simulated events with the goal to determine the beam polarization, $\vec{P}_B$. If the beam polarization vector

is directed arbitrary in the space, defined by x, y and z-coordinates, one can present it in the following way

$$\vec{P}_B = P_x\vec{x} + P_y\vec{y} + P_z\vec{z}, \tag{5}$$

where $P_{x,y,z}$ are the components of the beam polarization vector, $\vec{P}_B$, along the corresponding axis, while $\vec{x}, \vec{y}$ and $\vec{z}$ are the unit vectors (see Fig.2, right picture). The angular distribution of the "useful" photons from domain (3) is given by the relation

$$I(\theta, \phi) = I_0 \cdot [1 + \epsilon_n(\theta) \cdot cos\phi + \epsilon_s(\theta) \cdot sin\phi], \tag{6}$$

where θ and ϕ are the polar and azimuthal angles of the photons, $I_0(\theta)$ is the photon angular distribution for the unpolarized beam. We assume the full azimuthal acceptance of the PD. The asymmetries ϵ_n and ϵ_s depend (at a fixed photon energy) on the polar angle θ only and are the simple functions of the transverse components of the beam polarization and the analyzing power A_N, namely,

$$\epsilon_n = A_N \cdot P_y, \ \epsilon_s = -A_N \cdot P_x. \tag{7}$$

Assume that the EMC consists of the cells $(\Delta\theta)_i \times (\Delta\phi)_j$ and each cell detects $N(i,\ j)$ photons. At the fixed θ_i we sum up the events over the azimuthal cells j, that is

$$\epsilon_n(\theta_i) = \epsilon_n(i) = \frac{2}{N(i)} \cdot \sum_{j=1}^{n} N(i,j) cos\phi_j, \ \epsilon_s(\theta_i) = \epsilon_s(i) = -\frac{2}{N(i)} \cdot \sum_{j=1}^{n} N(i,j) sin\phi_j, \tag{8}$$

where $N(i) = \sum_{j=1}^{n} N(i,j)$.

Therefore, if the stable polarization vector is directed under the angle ϕ_0 to the normal to the horizontal plane (x,z), this angle can be defined for each cell through the relation

$$tg\phi_0 = \frac{\epsilon_s(i)}{\epsilon_n(i)}. \tag{9}$$

In order to get the result over a whole detector, we must take the weighted average over all cells. This is an important relation specially in the case when the experiment uses the longitudinally polarized proton beams and one needs to know whether we have any transverse component of the beam polarization. It means we must demonstrate with sufficient angular and statistical precisions that ϵ_n and ϵ_s are zeros. The additional checks can be done by switching on and off the Siberian Snakes, Rotators and Spin Flippers, as well as using the unpolarized beams.

4. Monte Carlo simulation

For convenience we choose the detector as divided into sectors on the polar and azimuthal angles. For generality we labeled earlier the polar angles by i and azimuthal angles by j. For the present application we select i=4 and j=4, so the number of cells is $4 \times 4 = 16$, as indicated in Fig.2 with the corresponding labels: the polar angles were labeled from the center to the perifery and the azimuthal angles from 30 to 90^0 in the clockwise direction starting from the x axis. Since we do not have the experimental data and should simulate them by FRITIOF program [9], we made the following assumptions:

- at any initial energy the analyzing power for domain (3) is equal to the one measured by E-704 Collaboration in the fixed target mode (FTM) at laboratory momentum of $p_L = 200$ GeV/c ($\sqrt{s} = 19.4$GeV);
- since the E-704 data are not complete (in the sense of presentation in x_F and p_T plots), we take the analytical formula for analyzing powers for the inclusive π^0 and η productions in the following way [10]:

$$A_N(x_A, p_T) = F(p_T) \cdot \{a_1 sin[a_7(x_A - a_2)] + a_6/s\}, \text{ for } x_A \geq a_4;$$
$$= F(p_T) \cdot \{a_1 sin[a_7(a_4 - a_2) + a_5(x_A - a_4)] + a_6/s\}, \text{ otherwise.} \quad (10)$$

Here $x_A = E/E_o$, where E is the energy of the produced particle, namely, π^0 or η, E_o is the beam energy. $F(p_T)$ is the QCD motivated function [11] taken in the form

$$F(p_T) = 2 \cdot p_T \cdot \frac{a_3}{(a_3^2 + p_T^2)}. \quad (11)$$

Parameters $a_1 \div a_7$ are free and they were determined by fitting expressions (10) and (11) to the published experimental data. They are presented below [10]:
for $\pi^0 : a_1 = 0.24 \pm 0.12,\ a_2 = 0.111 \pm 0.019,\ a_3 = 1.40 \pm 0.69,\ a_4 = a_5 = a_6 = a_7 = 0$;
for η-mesons: $a_1 = 1.00 \pm 0.36, a_2 = 0.323 \pm 0.048, a_3 = 1.00, a_4 = a_5 = a_6 = a_7 = 0$.

We assume that photons are produced with momentum $\vec{k}'$ in the production plane (see Fig.2, where $\vec{n}$ is a unit vector normal to the production plane directed at angle ϕ to the y axis). The polarization vector, $\vec{P}_B$, is aligned at the azimuthal angle, ϕ_0, to the y axis. Then the transverse components of the polarization vector are calculated through the relations:

$$P_y(i) = \frac{\epsilon_n(i)}{\bar{A_N}(i)} = \frac{\sum_j A_N(i,j) \cdot cos\phi_j}{\bar{A_N}(i)} \times \frac{2}{N(i)}, \quad (12)$$

$$P_x(i) = \frac{\epsilon_s(i)}{\bar{A_N}(i)} = \frac{\sum_j A_N(i,j) \cdot sin\phi_j}{\bar{A_N}(i)} \times \frac{2}{N(i)}. \quad (13)$$

Here the summation is taken over the azimuthal angles j at the fixed polar angle θ_i. We must average the defined beam polarization components over the indice i too.

Now let us look at the distributions calculated using Monte Carlo program FRITIOF-7.02 [9]. Fig.3 presents the photon distributions without a cut: a) the useful events versus $x_F(\gamma)$ for photons originated from π^0; b) the same for η. These two figures give the signal, s=2047 events; c) the "harmful" decay photons from π^0; d) the same for η; e) the background photons from other sources. These last three figures present the background, b=120264. It is seen that the essential part of background comes from the "harmful" π^0 (see Fig.3c).

If we take the ratio d = s/(s+b) we get d = $1.67 \cdot 10^{-2}$. In order to suppress the background, we must set an energy threshold for the detection of photons. Fig.4 shows the same distributions as in Fig.3, but after putting a cut $x_F(\gamma)$=0.4 (according to (3)). In this case the "harmful" photons are completely suppressed (for an ideal cut), photons from other sources are suppressed by a factor of ~ 10, while the useful photons are suppressed by a factor of ~ 3. Finally the dilution factor d becomes (539+100)/(539+100+208)= 0.76. This is an acceptable number. In each case (Fig.3 and Fig.4) the $5 \cdot 10^5$ events were generated. The study of the photon p_T distribution

shows (see Fig.5), that it is "harder"($\bar{p}_T = 0.55 - 0.58$ GeV/c) for the "useful" photons from η and π^0 (see Fig.5a and 5b) and softer for the background photons ($\bar{p}_T = 0.38$ GeV/c, see Fig.5c).

This is another direction for cutting backgrounds. Figs.5e and 5f show that the photon angles less than 2 mrad do not practically contain any useful events. It means that one can make a hole in PD with a radius ~ 45 mm. At the same time the outer size of detector is smaller than it should be (6 mrad is a geometrical acceptance of PD). It is necessary to look more attentively at this problem.

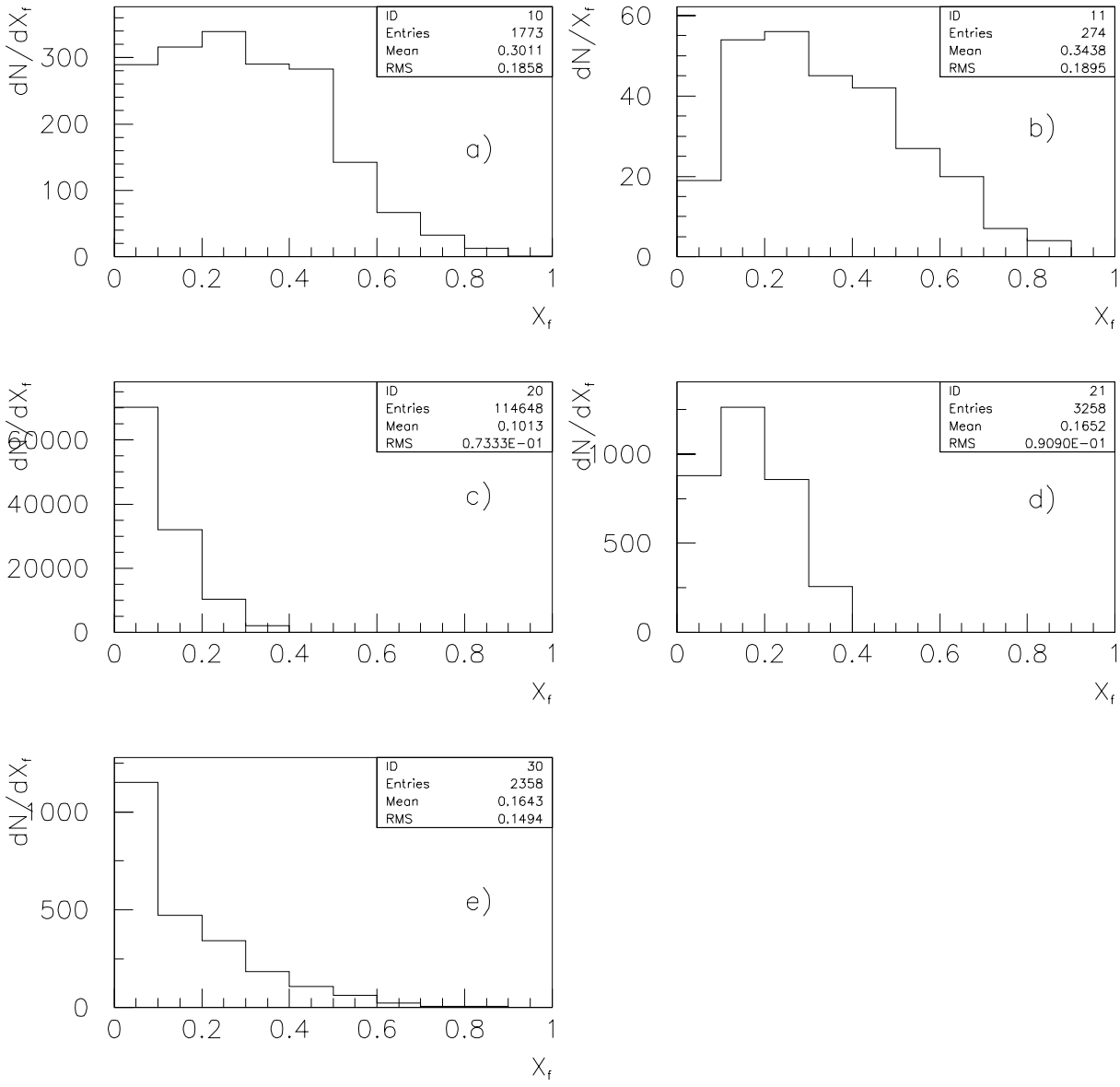

Fig. 3. The inclusive photon x_F distributions from pp-interaction at $\sqrt{s}$=500 GeV without a cut, photons from: a) the "useful" π^0 and b) η decays; c) the "harmfull" π^0 and d) η decays; e) other sources.

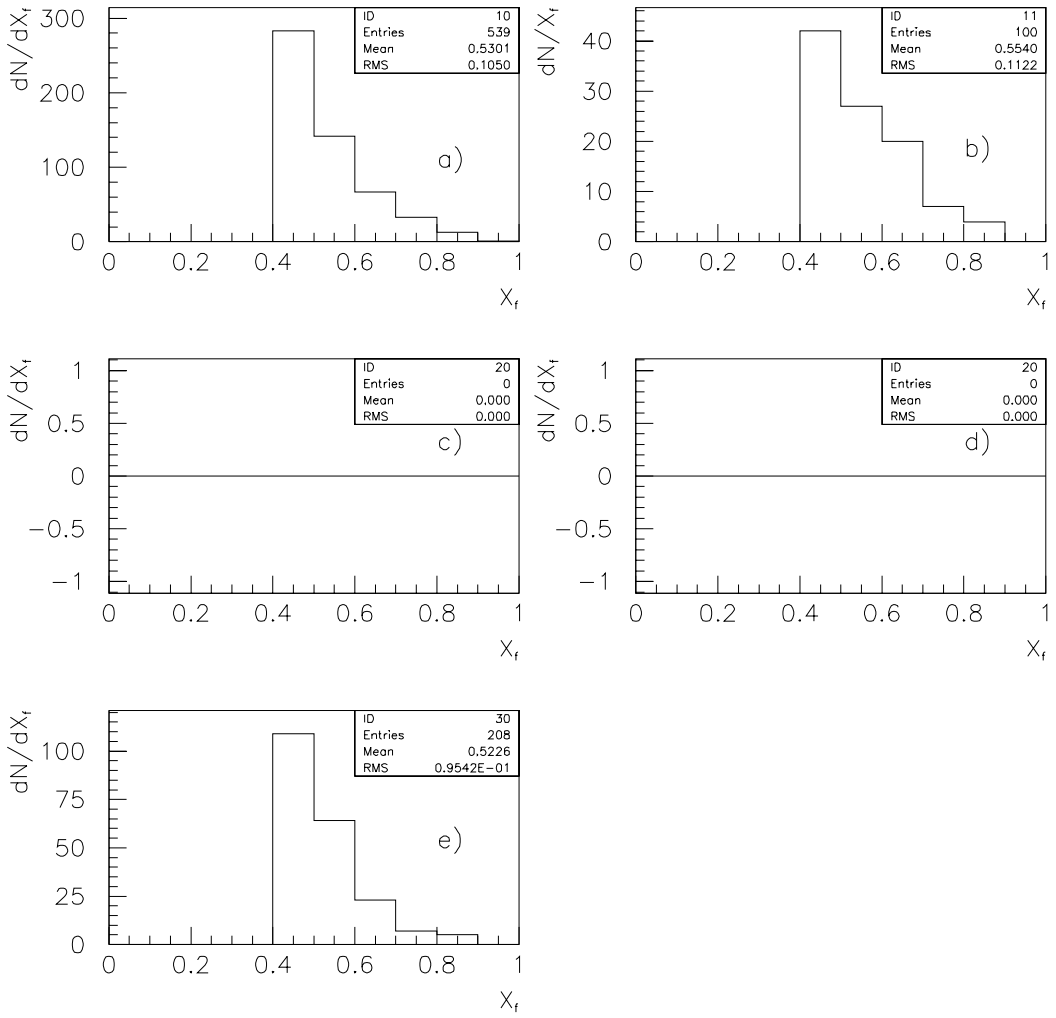

Fig. 4. The same as in Fig.3, but with a cut at $x_F(\gamma)$=0.4.

The analyzing power (numerator) for the decay photons from π^0 calculated according to formula (10) and in the denominator number of useful events for the same decays is presented in Table 1. Similar distributions for photons from η decays are presented in Table 2 while the background events are shown in Table 3.

Table 1. The analyzing power and number of photons from π^0-decays.

θ/ϕ^0	37.5	52.5	67.5	82.5
3	0.082/49	0.078/42	0.078/46	0.079/51
2	0.09/54	0.093/52	0.102/50	0.113/55
1	0.11/13	0.109/14	0.105/13	0.135/9

Table 2. The analyzing power and number of photons from η-decays.

θ/ϕ^0	37.5	52.5	67.5	82.5
4	0.09/12	0.09/24	0.10/17	0.10/23
3	0.10/21	0.10/14	0.10/14	0.11/27
2	0.12/16	0.10/11	0.11/11	0.10/6
1	0.11/6	0.12/5	0.11/4	0.11/8

Table 3. The backgrounds from other sources not π^0- and η-decays.

θ/ϕ^0	37.5	52.5	67.5	82.5
4	9	9	14	21
3	17	31	21	24
2	27	27	20	25
1	29	26	27	30

From Tables 1, 2, 3 and applying relation (5), one can estimate the beam polarization from the statistics coming from a quarter of PD

$$\bar{P}_B = 96.1 \pm 7\%, \tag{14}$$

which is consistent with the accepted value of the beam polarization, $P_B = 100\%$.

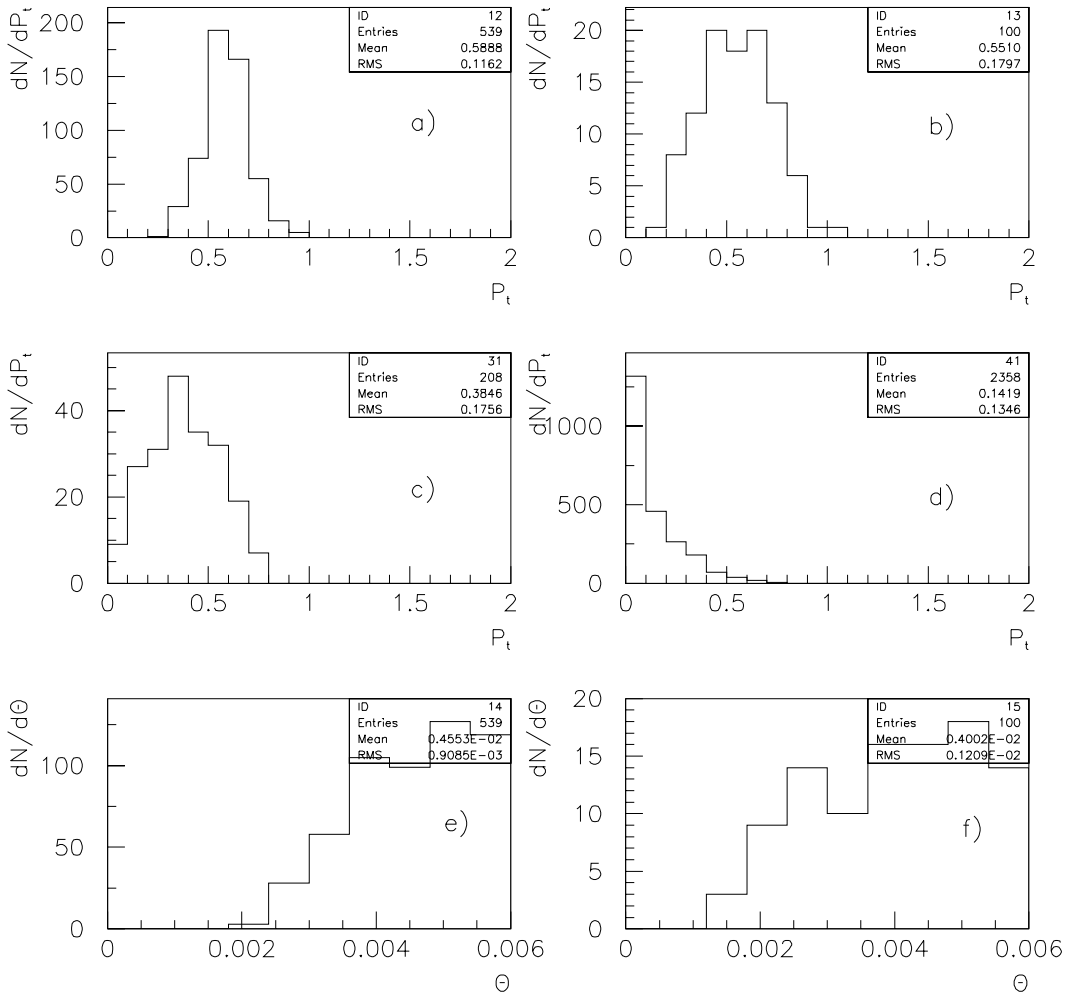

Fig.5. The p_t and θ distributions of photons emitted in pp interactions at $\sqrt{s}$=500 GeV with a cut at $x_F = 0.4$. The p_t distributions of photons from : a) π^0; b) η; c) other sources; d) other sources without cut. The angular θ distributions of photons (with a cut) in respect to the beam direction for: e) photons from π^0 decay, and f) photons from η decay.

In order to estimate the running time, we make the following calculations. The number of the generated events is $5 \cdot 10^6$, which corresponds to the total cross section σ_T around 60 mb. The number of the accepted good events in one quarter of the PD aperture is 448. It corresponds to the cross section $\Delta\sigma = (448/5 \cdot 10^6)\dot{\sigma}_T = 5.4$ μb. At the instantaneous luminosity of Ł = 10 $(\mu b)^{-1}$, we get the counting rate per second $\frac{dN}{dt} = 54$ cnts/sec. For a whole detector the counting rate will be 54·4 = 216 cnts/sec. The total number of the needed statistics, N, for reaching the precision $\delta P_B = 5\%$ is defined through the relation

$$N = \frac{1}{(A_N \cdot \delta P_B \cdot d)^2}, \tag{15}$$

where $A_N = 0.09$, $\delta P_B = 0.05$, $d = \frac{S}{S+B} = 0.6$ is the ratio of signal S to the sum of the signal and background, B. After putting all the numbers into (15), we get N=$1.4 \cdot 10^5$ events. Taking into account the counting rate 216 cnts/sec, we get the running time for collecting the necessary statistics, $T \approx 0.4$ hour. Assuming that $\eta-$decay also gives good events as π^0-decay, one can gain 20% time ib the polarization measurement.

5. The neutral hadronic backgrounds

At the collision of two proton beams a lot of neutral hadrons are produced and these hadrons interact with the photon detector. Depending on the deposited energy they may be detected by PD and dilute the photon analyzing power. The examples of such hadrons are the neutrons and K_L presented in Fig.6 for the $\sqrt{s} = 500$ GeV. The generated by PHYTHIA number of events were in both cases $5 \cdot 10^5$ so one can make a direct comparison with the number of photons (see Fig.3). By such comparison of Fig.6 (top right picture) and Fig.3a one may notice that the flux of K_L is bigger than that of the useful photons by a factor of $n(K_L) = \frac{5919}{1773} \times n(\gamma) = 3.3 \times n(\gamma)$. The mean energy and the energy spread of the K_L are $\bar{E}(K_L) = 57$ GeV and $\sigma_E(K_L) = \pm 40$ GeV, respectively, that is, similar to the ones for the useful photons without a cut, namely, $\bar{E}(\gamma) = 75$ GeV and $\sigma_E(\gamma) = \pm 46$ GeV.

Fig.6a shows the similar data for neutrons. In this case the neutron flux is much bigger, namely, $n(n) = \frac{110922}{1773} \times n(\gamma) = 63 \times n(\gamma)$. The mean energy and the energy spread equal $\bar{E}(n) = 118$ GeV and $\sigma_E(n) = \pm 50$ GeV, respectively. Therefore, the neutron flux may become a serious source of background in the detection of photons at almost zero degree. In order to make the numerical estimates of such background, we applied the GEANT utility to the geometry of PD as it is shown in Fig.1 and Fig.2. We assumed that the PD is a sandwich type calorimeter consisting of the Pb plate of 5 mm thick and the plastic scintillator of 2.5 mm thick. The total length of such sandwich is assumed to be x=22 X_0, where X_0 is a radiation length of the composite material. Since such length corresponds to the one interaction length, one expects that approximately 1/2 of the neutron flux will not interact with the PD.

The configuration of the vacuum pipes is complicated just in front of the PD. In calculations we took into account the materials of vacuum pipes (stainless steel), their diameter (5 inches, thickness — 2.5 mm). Besides we have assumed that there is a window of size 6×6 cm^2 in front of the PD 9 mm thick. All the neutral hadrons as well as photons were traced and their deposited energies in the PD were estimated.

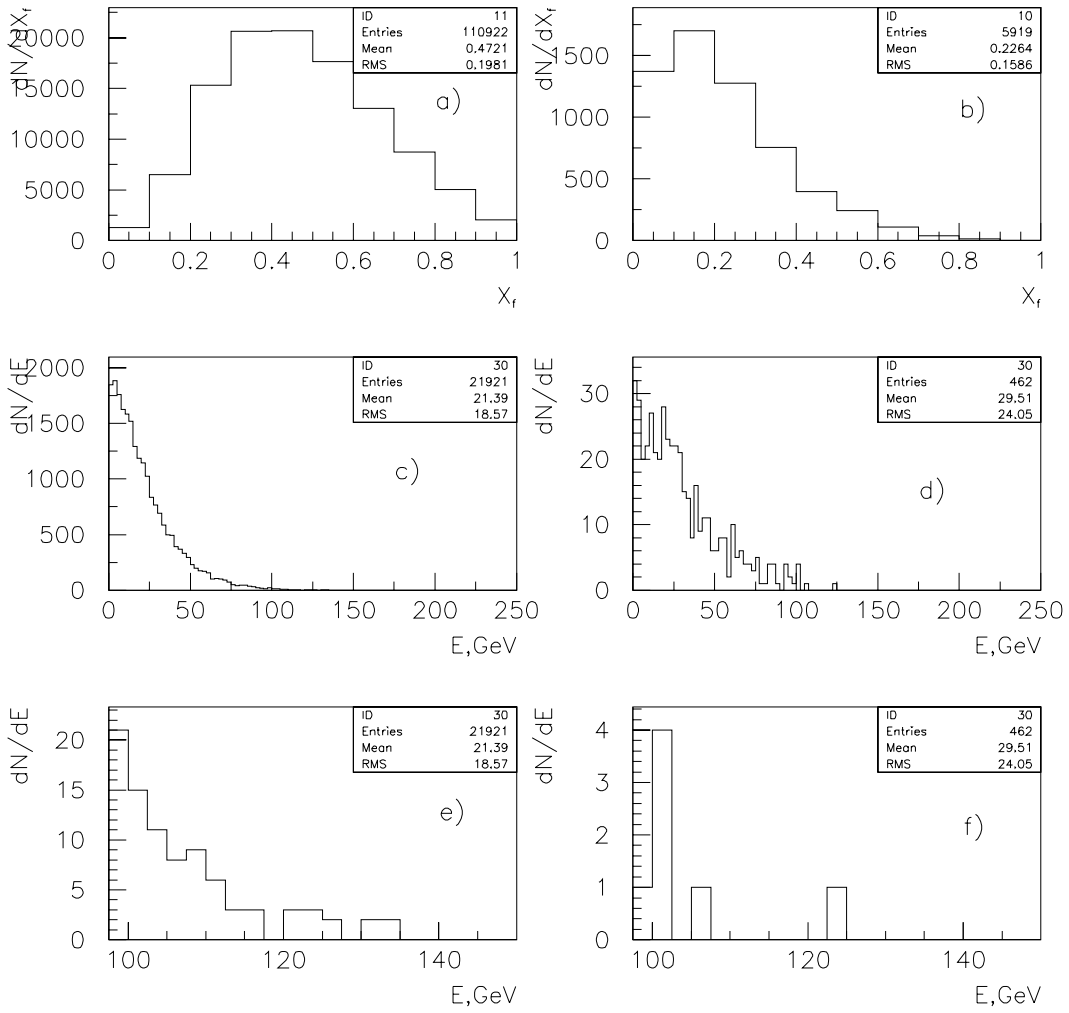

Fig. 6. The two top figures present the x_F distributions of neutrons (a) and kaons (b). The two middle figures present the energy deposited in PD by neutrons (c) and by kaons (d). The two bottom figures (e) and (f) show the enlarged tail part of the previous spectra, showing the amount of neutrons, and kaons, which can be detected by PD at fixed threshold. The pp-collision energy in c.m. $\sqrt{s} = 500$ GeV.

The obtained distribution for the deposited energy by neutrons (see Fig.6c) illustrates such an effect. The x-axis shows the energy deposited by neutrons in PD, while the y axis presents the number of neutrons. The mean deposited by neutrons energy is around 21 GeV, which is much smaller, than the threshold energy $E_{th} = 100$ GeV in the PD. In order to see how many neutrons can deposite the energy above the threshold one the next figure (Fig.6e) shows the expanded region bigger than 100 GeV. 92 of such neutrons were found. Similar estimate for K_L gives 6 of such events (see Fig.6f). In total we expect to have 98 neutral hadrons contributing as a background. Therefore, the total number of backrounds arising from harmful photons (70 events, Fig.7b) and neutral hadrons (98 events) is equal to 168 events. Since the number of useful photons equals 347 events (Fig.7a), we have the signal to signal + background ratio d=0.67. Applying relation (15) to $\delta P/P = 5\%$, we conclude that one needs to accumulate N=$1.1 \cdot 10^5$, events which requires the running time of order T=0.25 hr. This still seems tolerable.

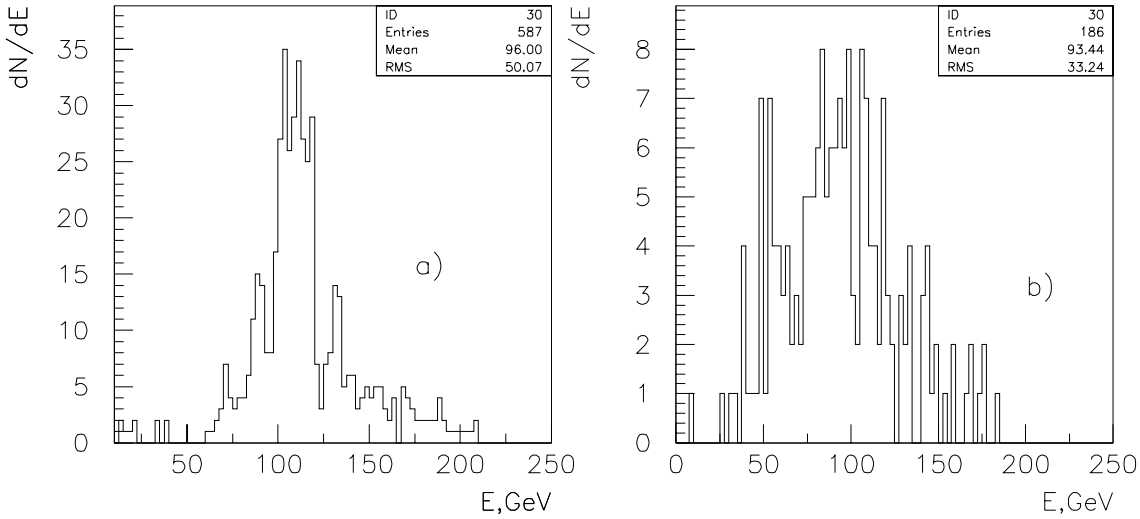

Fig. 7. The energies deposited in PD by the useful (left picture) and background (right picture) photons.

6. The beam-gas interaction

The next source of background contributing to the photon analyzing power is an interaction of the beam with a gas in the vacuum pipe. This interaction is not local but distributed over a long distance. We have assumed that this region is limited by the centers of two DX magnets flanking the straight section . This distance is equal to $l_T = 23.1$ m. Then, the beam-gas luminosity is estimated through the relation

$$L = n_b \cdot N_B \cdot n_T \cdot l_T \cdot f_0 \cdot q, \tag{16}$$

where $n_b = 120$ and $N_B = 2 \cdot 10^{11}$ are the number of bunches and the number of protons in a bunch, respectively, n_T and l_T are the gas density and the length of interacting target, q is the factor of the beam and gas overlapping, f_0=78 kHz the beam circulation frequency. In our case q=1, while the gas density can be estimated by the relation

$$n_T = \frac{P}{k \cdot T} = 9.656 \cdot 10^{18} \cdot \frac{P(Torr)}{T(Kelvin)}, \tag{17}$$

where P and T are the gas pressure and temperature inside the vacuum pipe, respectively. Since the beam-gas interaction occurs in the warm section of RHIC, therefore $P = 5 \cdot 10^{-5}$ Torr, T=300 K, and we get a gas density $n_T = 1.6 \cdot 10^7$ mol/cm^3. Now we can estimate the beam-gas luminosity

$$L_{bg} = 120 \times 2 \cdot 10^{11} \times 1.6 \cdot 10^7 \times 23.1 \cdot 10^2 \times 7.8 \cdot 10^4 = 6.9 \cdot 10^{28} \text{ cm}^{-2}\text{sec}^{-1}. \tag{18}$$

In a similar way one can estimate the luminosity for the beam-polarized jet target interactions, $L_{bj} = 1.9 \cdot 10^{30}$ cm^{-2}sec^{-1} and for the beam-cluster target interactions, $L_{bc} = 3 \cdot 10^{32}$ cm^{-2}sec^{-1}. For the estimation of the collision rates for each of the discussed above cases, one needs to determine the inelastic scattering cross sections, correspondingly.

The internal gas in the vacuum pipe consists of three components [13]: hydrogen molecules $H_2(50\%)$, molecules of methane $CH_4(5\%)$ and molecules of dioxide carbons $CO(5\%)$.

We should calculate the inelastic interaction cross sections for three cases, respectively $\sigma_{in}(pH_2), \sigma_{in}(pCH_4)$ and $\sigma_{in}(CO)$. The first cross section is defined as $\sigma_{in}(pH_2) = 2 \cdot \sigma_{in}(pp) = 2 \times 33$ mb=66 mb. The following cross sections are defined for proton-nuclei interactions:

$$\sigma_{in}(pCH_4) = \pi \times [1.2(1^{1/3} + 12^{1/3} + 4^{1/3}]^2 \cdot 10^{-26} \text{ cm}^2 = 1076 \text{ mb},$$
$$\sigma_{in}(pCO) = \pi \times [1.2(1^{1/3} + 12^{1/3} + 16^{1/3}]^2 \cdot 10^{-26} \text{ cm}^2 = 1525 \text{ mb}. \quad (19)$$

Therefore, the resulting cross section for the beam-gas interaction is $\sigma_{in}(bg) = 189$ mb. So, the beam-gas and the beam-polarized jet interaction rates equal

$$\dot{N}_{bg} = L_{bg} \times \sigma_{in}(bg) = 6.9 \cdot 10^{28} \times 189 \cdot 10^{-27} = 1.3 \cdot 10^4 \text{ sec}^{-1},$$
$$\dot{N}_{bj} = L_{bj} \times \sigma_{in}(beam - polar.jet) = 1.9 \cdot 10^{30} \times 33 \cdot 10^{-27} = 6.3 \cdot 10^4 \text{ sec}^{-1}. \quad (20)$$

The ratio of rates $\frac{\dot{N_{bg}}}{\dot{N_{bj}}}$=0.21, while the dilution factor becomes equal to d=$\frac{\dot{N_{bg}}}{\dot{N_{bg}}+\dot{N_{bj}}}$=0.17. For the case of the cluster target as well as for the case of two polarized beams collision this number is much smaller (around 0.001-0.002) due to the higher luminosities.

There is a technique for suppression the background from the beam-gas interaction. This is a vertex reconstruction detector registrating the charged particles accompanying the useful photon production. Assume we catch these charged particles by the tracking detector (for example, the cathode strip chambers (CSC in Fig.1) with a full azimuthal coverage) with an internal radius $r_{ir} = 7$ cm and an outer radius $r_{or} = 11$ cm and installed at the distance around 5.5 m from the interaction point. According to the estimates by FRITIOF program for the configuration of detectors presented in Fig.1 at $\sqrt{s}$=500 GeV 60% of useful photons will be accompanied by the charged particles. In order to estimate the vertex reconstruction precision, $\pm x0$, along the beam direction, let us take the worst case, when the charged particles are detected at the smallest emitting angles. Assume we use the two extreme planes of the CSC's with coordinates x1=5 m, y1=70 mm and x2=6m, y2=84 mm. For the coordinate resolution of CSC $\delta = 0.1$ mm, we get the relation

$$\pm\, x0 = \frac{x1 \cdot y2 - x2 \cdot y1 \pm \delta \cdot (x1 + x2)}{y2 - y1 \pm 2\delta}. \quad (21)$$

For the ideal detector alignment the first two terms in the numerator cancel each other and it leads to the simple relation used for the estimate of x0

$$\pm\, x0 = \delta \cdot \frac{x1 + x2}{y2 - y1 \pm 2 \cdot \delta}. \quad (22)$$

Since we have all the necessary numerical values we can estimate $x0 = \pm 8$ cm. For 3 $\sigma = 30$ cm, one can restrict the region of the beam gas interaction to around 1 m. Therefore, instead of 23 m we have now 1 m interaction region and the backgrounds from the beam gas interaction might be suppressed by a factor of 10. Sure, one needs to take the optimum shape of the vacuum pipe for our goal.

7. The LIPP calibration

Above we discussed the case when the collider mode ($\sqrt{s} = 500$ GeV) was running. If one assumes, that both proton beams are longitudinally polarized, then Photon Detector may only permanently check the absence of any essential transverse component of the beam polarization.

If such a component arises for some reason, one can detect it and use later this information for the correction of the experimental data. Also the PD allows one to define the inclination of the polarization vector at the IP with respect to the horizontal (vertical) plane. The precision in such measurement depends on the two factors: the PD angular resolution and statistics. According to our crude segmentation of PD ($\Delta\varphi = 15^0$) we expect to have one sigma resolution $\sigma(\varphi) = 15/\sqrt{12} \approx 4.3^0$. It corresponds to the appearence of the horizontal component of the polarization vector of order 7%. If one reaches the statistical precision of order 5% (see above), therefore, one can say that the 3 sigma declination of the polarization from the vertical plane can be surely detected.

Above we also discussed the case where one out of two beams was normally polarized with 100% polarization. We estimated the running time for reaching 5% precision in the beam polarization measurements. In this case we made two crucial approximations:

1. Assume the applicability in this case ($\sqrt{s}$=500 GeV) E704 data on the analyzing power, $A_N(\pi^0)$, obtained at energy $\sqrt{s}$=19.4 GeV.
2. Assume the applicability of relation (10).

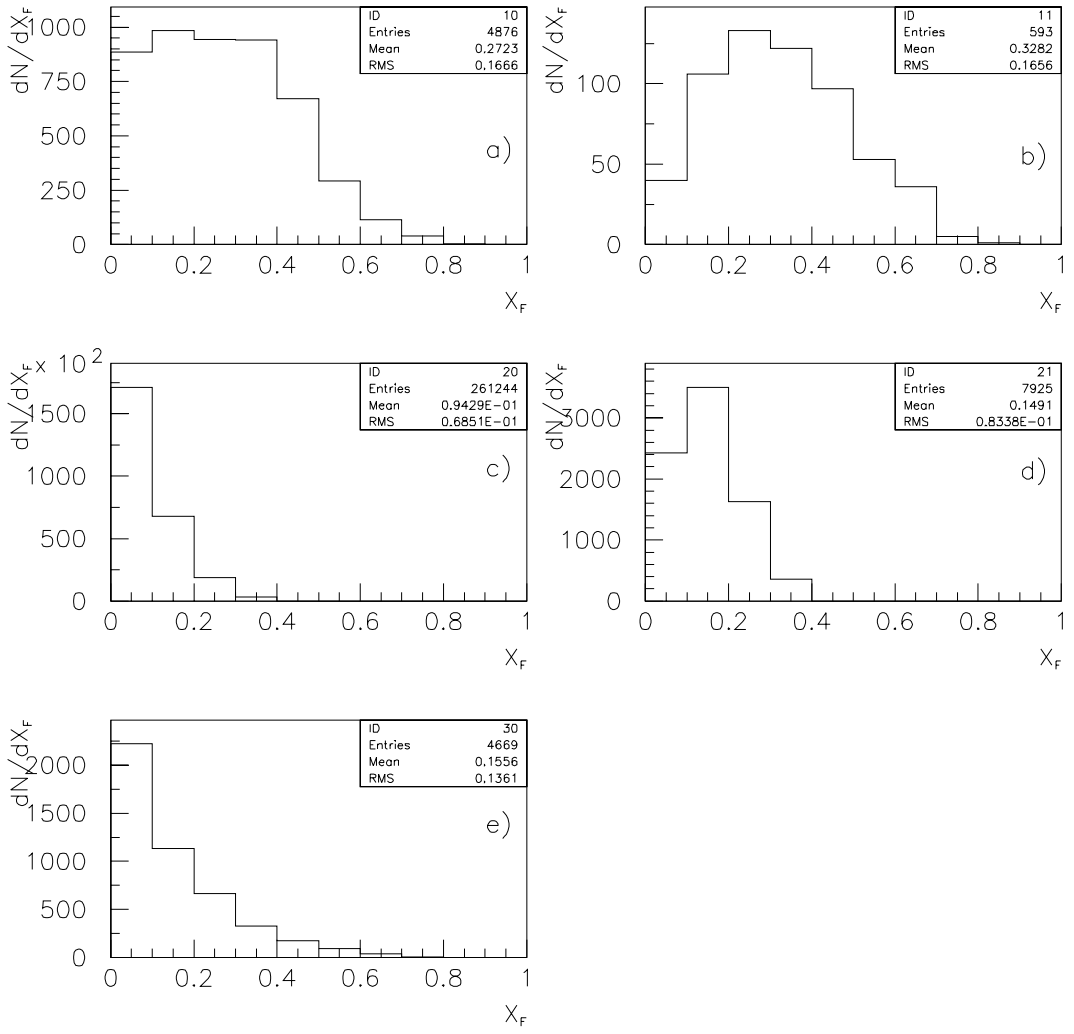

Fig.8. The x_F distributions of photons in pp collisions at $\sqrt{s}$=19.4 GeV (calibration run). The useful photons from: a) π^0; b) η-mesons; harmful photons from: c) π^0, d) η-mesons, c) from other sources.

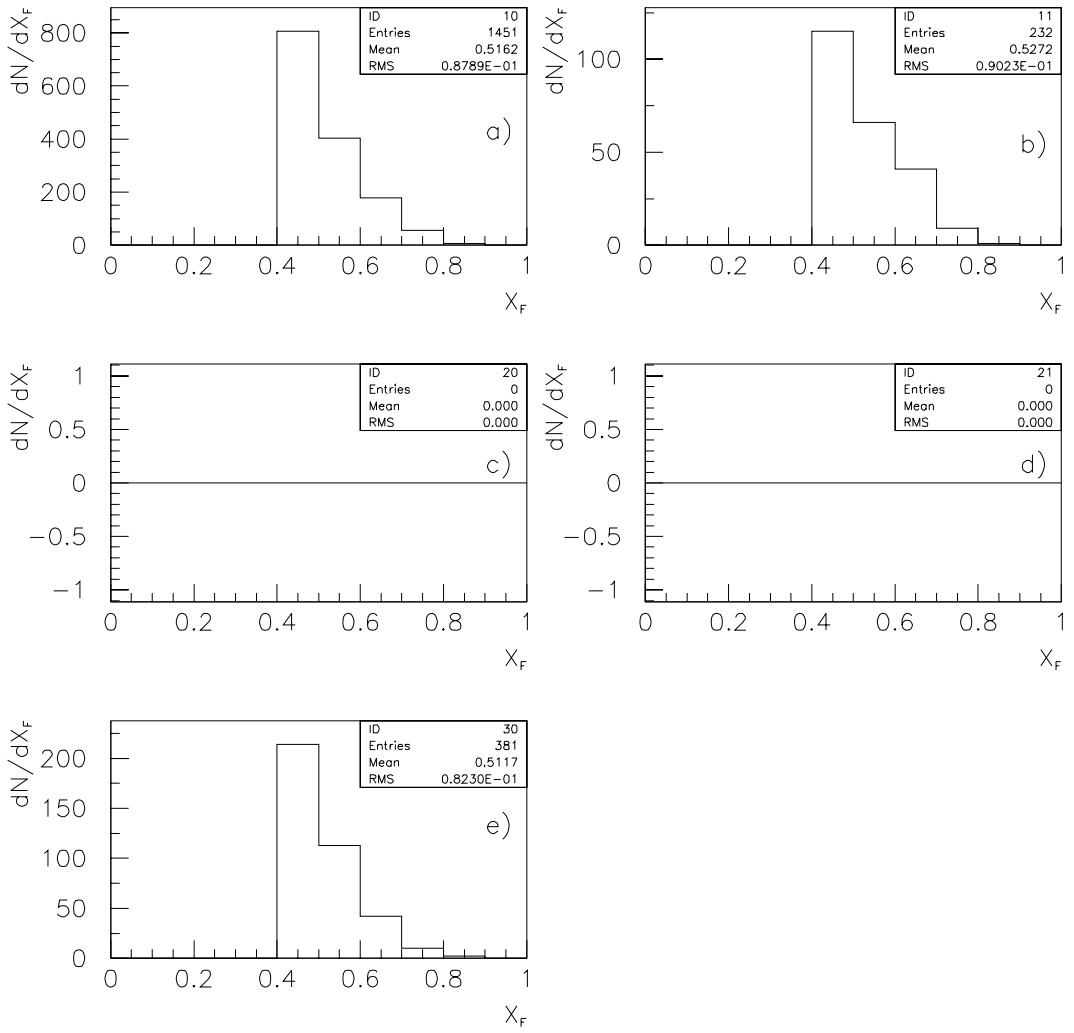

Fig. 9. The same as in Fig.8 but with a threshold at $x_F(\gamma)$=0.4.

In order to overcome these approximations, we propose a calibration experiment similar to E704. For that we put the Internal Target (IT) at a distance of 8.63 m from IP (see Figs.1). Assuming that the beam polarization at $p_{lab} = 200$ GeV/c was established with a good precision by some known technique [1], we measure the analyzing power of the inclusive photon production with a necessary accuracy. In such a way one can check relation (10) and improve the fit parameters. Then, we return to the collider mode, where at least one of the beam is polarized and check our first assumption above.

We applied FRITIOF — 7.02 program [9] to this calibration scheme and got the results presented in Figs.8 and 9. The $5 \cdot 10^6$ events were generated. The number of useful events is: $N_u(\pi^0) = 4.8{\cdot}10^3$ (Fig.8a) , $N_u(\eta) = 5.9{\cdot}10^2$ (Fig.8b) . The main background, $N_b(\pi^0) = 2.6{\cdot}10^5$, comes from the soft π^0 decays (see Fig.8c), while the backgrounds from η decays, $N_b(\eta) = 7.9 \cdot 10^3$, (Fig.8d) and other sources, $N_b(\text{others}) = 4.7 \cdot 10^3$, (Fig.8e). Therefore, the signal to signal + background ratio is, $d = s/s+b = (4876+593)/(4876+593+261244+4669) = 2 \cdot 10^{-2}$. After introducing a cut $x_F = 0.4$ we get (see Fig.9), $d = (1451+232)/(145+232+381) = 0.815$.

A counting rate can be estimated by the way, we used before. At first, the detectable cross section is $\Delta\sigma = 1683/5 \cdot 10^6 \sigma_T = 0.34 \times 60 \cdot \mu$b=20 μb. Assuming that the luminosity is 10 μb^{-1} we get the counting rate, $\dot{N}$(cal.run)= $20 \cdot 10 = 200$ cnts/sec for one quarter of the PD. Taking into account an average analyzing power, $\overline{A}_N = 0.09, d = 0.815$ (see Tables 4, 5, and 6), $P_B = 0.05$, one gets a running time ≈ 15 min.

Table 4. The analyzing power and number of photons from π^0-decays in the calibration run.

θ/ϕ^0	37.5	52.5	67.5	82.5
4	0.077/19	0.08/24	0.08/19	0.078/24
3	0.09/302	0.08/308	0.08/298	0.085/280
2	0.1/404	0.1/394	0.1/370	0.1/389
1	0.12/1	0.11/1	0.11/1	0.13/1

Table 5. The analyzing power and the number of photons from η-decays in the calibration run.

θ/ϕ^0	37.5	52.5	67.5	82.5
4	0.10/7	0.08/4	0.08/5	0.07/3
3	0.08/50	0.08/38	0.09/41	0.09/52
2	0.10/40	0.10/60	0.11/49	0.10/48
1	0.12/4	0.11/6	0.12/10	0.13/6

Table 6. The backgrounds from other sources than π^0- and η-decays in calibration run.

θ/ϕ^0	37.5	52.5	67.5	82.5
4	5	1	3	3
3	15	22	19	14
2	61	83	71	68
1	43	58	53	56

Conclusions

It is proposed to build the local inclusive photon polarimeter for continuous monitoring the beam polarization at the interaction point at the RHIC top energy. Such polarimeter will evidently work at a fixed target mode and, in case of a weak energy dependence of the analyzing power, in the colliding mode as well. A full azimuthal coverage allows one to measure the stable polarization direction at the interaction point. Possible background sources were revealed and the techniques to suppress the backgrounds are proposed. The high counting rate permits one to reach a statistical accuracy of order 5% in a reasonable time.

Acknowledgements

We would like to thank V.S.Datsko, V.M. Emelyanov, Y. Goto, K. Imai, A. Penzo, N. Saito, O.V. Selyugin and D. Underwood for the stimulating discussions.

References

[1] Y. Makdisi, in *Proc. 12th Int. Symp. on High-Energy Spin Physics,* eds. C.W. de Jager *et al.,* (World Scientific, Singapore, 1996), p.107.

[2] T.Roser, in: *Proc. of 13th Int. Symp. on High-Energy Spin Physics,* eds. N.E. Tyurin *et al., (World Scientific, Singapore, 1998), p.182.*

[3] K. Imai, in: *Proc.of Workshop RHIC SPIN*, Riken BNL Research Center, October 6-8, 1999, p.251.

[4] D.P. Morrison for the PHENIX Collaboration, *Nucl. Phys.* A638 (1998) 565.

[5] RHIC Design Manual, revised version, April 1998, p.WBS 1.8.10.

[6] A.A. Bogdanov et al., *The Inclusive Neutral Pion Polarimeter for High Energy Accelerators/Colliders*, preprint IHEP 98-54, Protvino, 1998.

[7] E.A. Andreeva et al., *The Inclusive Neutral Pion Polarimeter for RHIC*, preprint IHEP 97-61, Protvino, 1997.

[8] D. Besset et al., *Nucl. Instr. and Meth.* 166 (1979) 513.

[9] Hong Pi, *Comp. Phys. Comm.* 71 (1992) 173.

[10] V.V. Abramov, *Eur. Phys. J.* C14 (2000) 427.

[11] G. Kane, J. Pumplin, and W. Repko, *Phys. Rev. Lett.* 41 (1976) 1698.

[12] H.-U. Bengtsson and T. Sjöstrand, *Computer Physics Commun.* 46 (1987) 43.

[13] D. Trbojevie, in: Proc. of Workshop on Jet Targets ar RHIC, January 21-28, 2000, BNL.

Received October 12, 2000

А.А.Богданов, С.Б.Нурушев, М.Ф.Рунцо и др.
Локальный инклюзивный фотонный поляриметр для RHIC.

Оригинал-макет подготовлен с помощью системы LaTeX.
Редактор Е.Н.Горина. Технический редактор Н.В.Орлова.

Подписано к печати 24.10.2000. Формат 60 × 84/8. Офсетная печать.
Печ.л. 2.12. Уч.-изд.л. 1.6. Тираж 160. Заказ 224. Индекс 3649.
ЛР №020498 17.04.97.

ГНЦ РФ Институт физики высоких энергий
142284, Протвино Московской обл.

Индекс 3649

П Р Е П Р И Н Т 2000-42, И Ф В Э, 2000